APPLICATION OF A MODIFIED DIFFRACTION STACK FOR THE LOCALIZATION OF MICROTREMOR DATA

D. Anikiev, D. Gajewski, B. Kashtan, E. Tessmer, C. Vanelle

email: *danikiev@earth.phys.spbu.ru*

keywords: *Diffraction stacking, non-stationary data, low frequency events, microtremors*

ABSTRACT

It was demonstrated previously that the localization of acoustic emissions generated by, e.g., hydraulic injection, can be successfully performed using a modified diffraction stack. This conclusion also holds for strongly heterogeneous media and for a sparse distribution of receivers. Recently, the observation of microtremor data was proposed as a direct hydrocarbon indicator. These data are, however, much lower in frequency content than acoustic emissions. Applying the stacking technique to low frequency microtremor data indicates limitations of this method. The applicability of the ray method may be violated for strongly heterogeneous media and low frequency data. Such data are strongly affected by triplications and the interference of arrivals. The strongest events are not attributed to the first arrival but to later arrivals. Moreover, the moveout of these interfering high energy later arrivals is also different with respect to the first arrival. This leads to a focussing of the energy at a wrong depth position if high frequency ray theory first arrival traveltimes are used to determine stacking trajectories. This holds if the correct velocity model is used for the localization of the low frequency data. Localization of seismic events by the modified diffraction stack is very well applicable to high frequency data like acoustic emissions. For the localization of low frequency data, or more precisely, for data from environments where the spatial wavelength of heterogeneities is smaller than the prevailing wavelength of the signal, full wave form techniques like the reverse modeling approach give better results.

INTRODUCTION

The passive seismic method gains considerable momentum in the hydrocarbon industry. Locating passive seismic events is a new technology for reservoir monitoring or direct observations of hydro-frac generation. The localization of seismic events is a fundamental problem for passive seismic observations. New techniques to localize acoustic emissions, i.e., events generated by hydraulic injections or hydro-fracing, were recently suggested. These methods do not require arrival picking (Gajewski and Tessmer, 2005; Rentsch et al., 2007; Gajewski et al., 2007). Another advantage of these techniques which rely on back projection of energy recorded in the observing network is the focussing of events. This increases the detection level for localization of weak seismicity. In this paper we apply the localization technique using a stacking approach to backproject passive seismic observations (Anikiev et al., 2006, 2007; Gajewski et al., 2007). In this approach the subsurface is discretized and each subsurface location is considered to be a potential location of a seismic event. A velocity model is assumed and the diffraction traveltimes for each subsurface location are determined. These traveltime trajectories are used for stacking. Since the event time (i.e., zero time) is not known in passive seismic studies the trajectory is moved through the whole time window of the data under consideration and stacked for each time. The stack result is squared and forms the value of the so called image function for this location. The source location corresponds to the position of the maximum of the image function. For further details on the method we refere to Anikiev et al. (2006, 2007); Gajewski et al. (2007) In this paper we apply the localization approach to backproject microtremor data , i.e., low frequency non-stationary seismic data.

Such data were suggested as a direct hydrocarbon indicator. Using passive seismic surface observations low frequency spectral anomalies between 1-4 Hz were observed above the reservoir area but not outside of it (see, e.g., Graf et al., 2007). It is speculated that these low frequency non stationary seismic signals are a result of resonant oscillations of oil within the porous reservoir. Whether the spectral anomalies really originate from the reservoir was not clear. Therefore Steiner et al. (2008b) applied the reverse modeling technique of Gajewski and Tessmer (2005) to backproject the mircotremor observations to the subsurface. In a synthetic and real data case study these authors obtained images showing a focussing of energy in the reservoir area and therefore concluded that the microtremors in fact originated from the reservoir. The images generated by these authors are contaminated by noise at the near surface. This is inherent to the reverse modeling approach, since the amplitudes are always strongest at the receivers if no compensation of spreading losses is applied and if a small number of receivers is used. It was also necessary to apply a special imaging condition in order to enhance the weak energy of the microtremors. This motivated us to apply the localization method based on a stacking approach also to low frequency microtremor data.

Since a complex velocity model was considered by Steiner et al. (2008b) we first investigate the influence of the prevailing signal frequency of stationary seismic events (i.e., acoustic emissions) on the localization for this model. In the first part we study the localization of high frequency acoustic emissions for a complex velocity model and a sparse receiver distribution. We further investigate its performance on low frequency stationary data, i.e., low frequency seismic emissions. This was a prerequisite since the synthetic microtremor data were generated for the complex model and low frequencies. In the second part of the paper we apply the localization method to microtremor data. Acoustic and elastic representations of the complex model are considered for both parts of the study.

VELOCITY MODEL

The velocity model used by Steiner et al. (2008b) is reproduced in Fig. 1. The green and blue colors represent sedimentary layers of P-wave velocities between 1200 and 3000 km/s with a constant density of 2000 kg/m^3. Velocities of about 6000 km/s indicate the crystalline basin with a density of 3000 kg/m^3. The computational grid for the modeling consits of 901 nodes in horizontal direction and 301 nodes in vertical direction with a spacing of 10 m between nodes. Absorbing layers of 500 m width are introduced to avoid reflections from the model boundaries. The area of the reservoir is indicated by black lines. It is about 50 m thick and 2 km long. For the elastic case the S-wave velocities are determined from P-wave velocities by application of a factor of $1/\sqrt{2}$. This implies $\lambda = 0$ if the elastic properties of the medium are described by Lame-Parameters λ and μ.

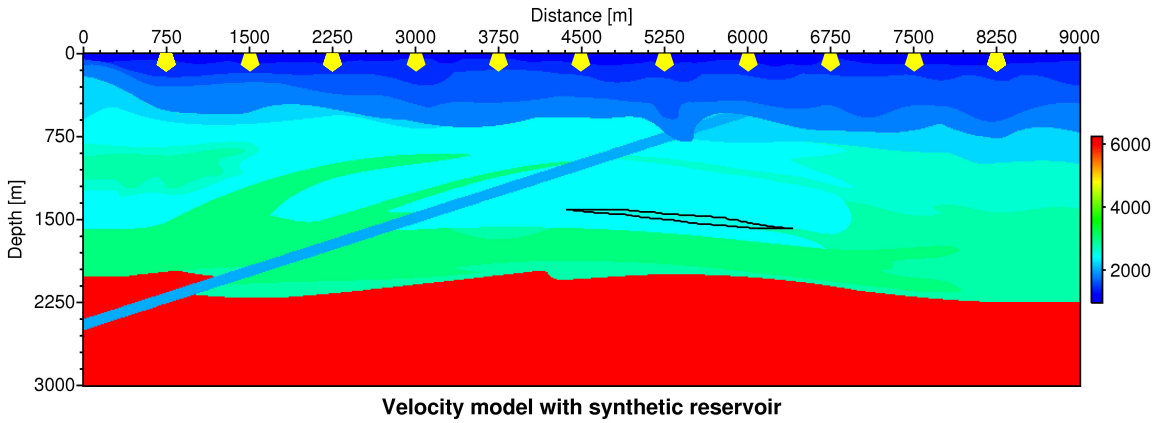

Figure 1: The velocity model and acquisition scheme. The colour legend on the right shows P-wave velocities in m/s. The recording network of the synthetic experiment consists of 11 receivers at the surface with a 750 m spacing indicated by yellow colors. The reservoir area is a thin zone indicated by black lines.

TRAVELTIMES

In all localization studies we assume that the velocity model is known. A finite difference (FD) eikonal solver (Vidale, 1988; Leidenfrost et al., 1999) was used to generate traveltimes for the above described model (see Fig. 1). Results of traveltime computations for source positions at 0.75 km, 4.5 km and 6.0 km are shown in Figs. 2, 3, 4, respectively. Since no smoothing was applied to the velocity model the traveltime contours display some roughness in areas of strong velocity variations.

Traveltimes to all subsurface locations were computed for source locations at the 11 considered receiver positions. The traveltimes from source locations in the subsurface to the 11 receivers are obtained by resorting and assuming reciprocity. Since the velocity model was not smoothed this assumption might not be applicable everywhere. It is, however, expected that the effect on the localization is negligible since random traveltime errors will only affect the total amplitude of the stacked energy, i.e., the final value of the image function but not the location of the maximum.

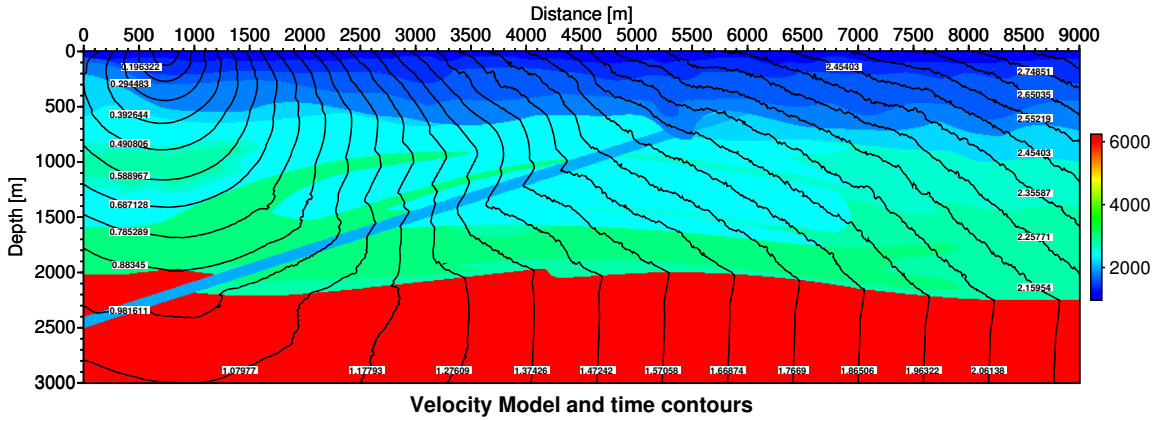

Figure 2: Velocity model and traveltime time contours for a source at 750 m.

LOCALIZATION OF ACOUSTIC EMISSIONS

Acoustic emissions might be generated by hydraulic, CO_2 or steam injection. Such injections are carried out for enhanced oil recovery or CO_2 sequestration. Acoustic emissions may also represent production noise by retrieving oil or gas from the reservoir. The events are usually characterized by high frequencies generated from point dislocation sources. Anikiev et al. (2007); Gajewski et al. (2007) have shown, that the stacking method is a suitable tool to locate such events even when the signal-to-noise (S/N) ratio is rather poor. Prior to the application of the method to microtremor data we need to study its performance for complex models and sparse receiver networks as well as its dependence on the frequency content of the data. For this purpose we consider the model of Fig. 1 and a point source at x=5000 m and z=1500 m. Acoustic and elastic wavefields are generated using a pseudospectral modeling method (Kosloff and Baysal, 1982; Reshef et al., 1988) and a time step of 0.5 ms with a total time of 4 s. We first consider the acoustic case.

Acoustic case

Seismograms for the acoustic modeling are shown in Figures 5, 6. A Ricker signal (second derivative of Gaussian) is used as source time function. We consider cut off frequencies of 60 and 30 Hz, representing the spectral content of acoustic emissions observed at the surface and a signal with a cut off frequency of 4.5 Hz representing the spectral content of a microtremor signal. The prevailing frequencies in the considered events are about half the cut off frequency. For the discussion of these figures we have to keep in mind that traveltimes obtained by ray tracing or FD Eikonal solvers correspond to traveltimes for $\omega \rightarrow \infty$, i.e., the

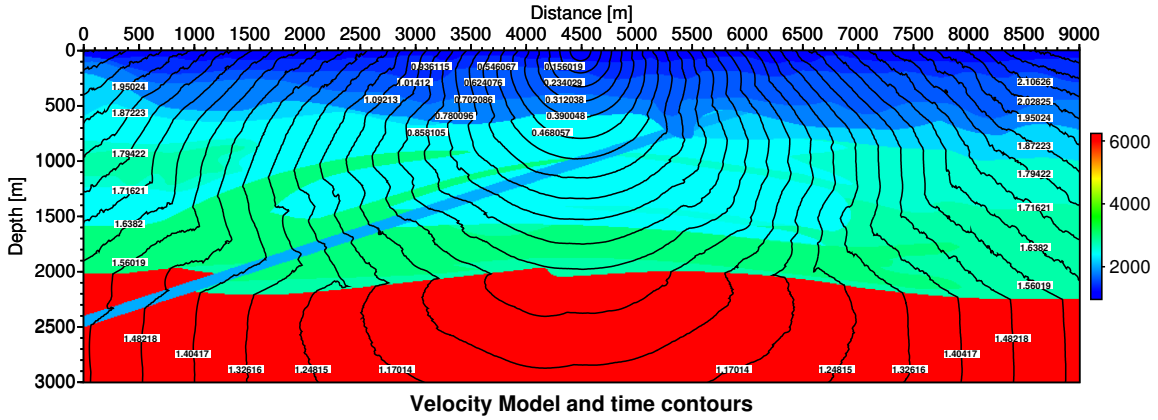

Figure 3: Velocity model and traveltime time contours for a source at 4500 m.

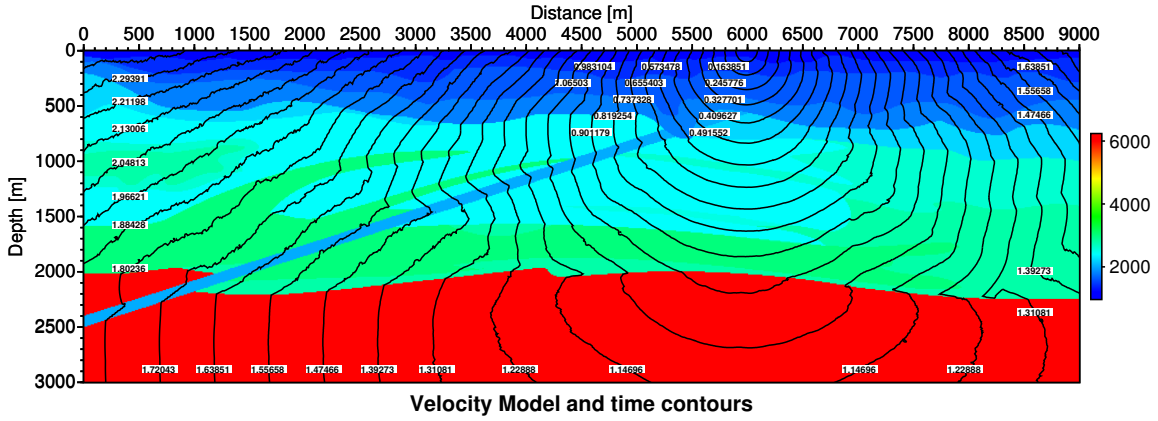

Figure 4: Velocity model and traveltime time contours for a source at 6000 m.

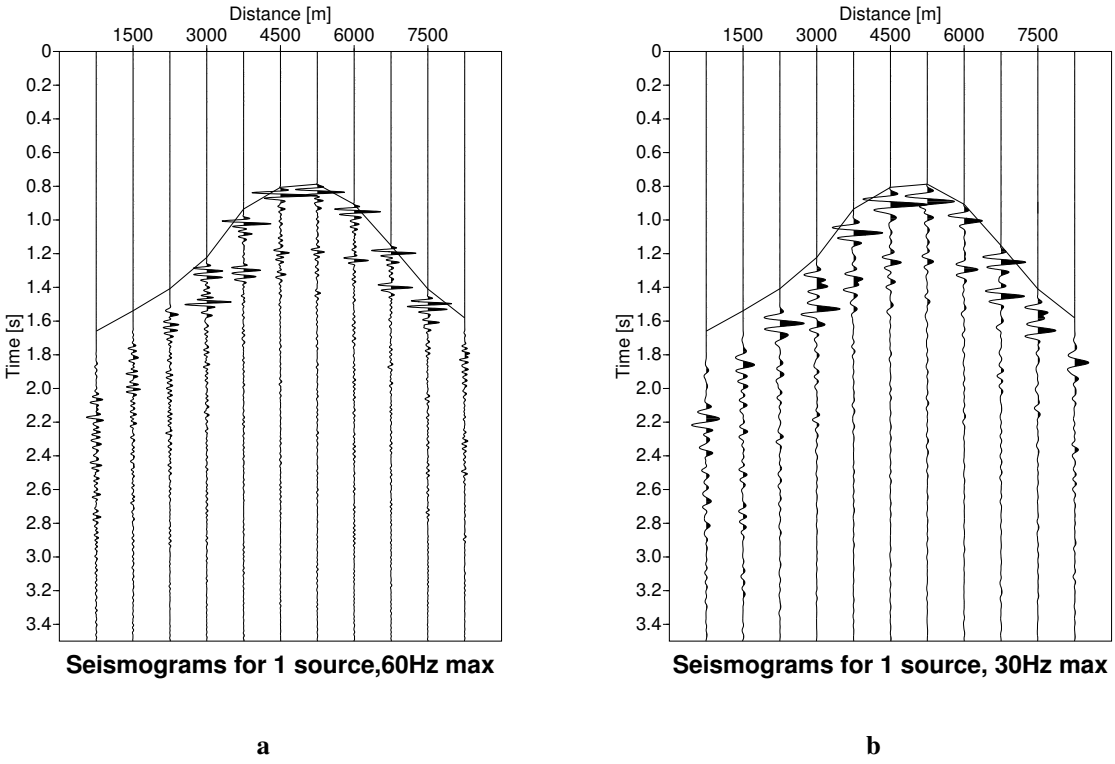

Figure 5: Seismograms for a point source in the acoustic heterogeneous medium (see Fig. 1). A Ricker signal is used as source time function with 60 Hz (a) and 30 Hz (b) cut off frequency. First arrival traveltime curves for the correct source position and source time are also shown.

traveltimes are high frequency (HF) traveltimes. More precisely, it is assumed that the spatial variations in the model are small compared to the prevailing wavelength of the signal. More general this means that all variations in velocity, amplitude, polarization, slowness are small compared to a characteristic length l (Červený, 2001). Assuming an average velocity of 2100 m/s in the sediments the prevailing wavelength of the considered 60, 30 and 4.5 Hz cut off frequency signals is about 70, 140, 933 m respectively.

Moreover, for FD eikonal solvers the computed traveltimes are not only HF traveltimes but always correspond to the first arrival traveltimes, i.e., to the fastest propagating wave. In complex media, the fastest propagating wave is not necessarily the most energetic arrival since we have triplications. This is well known from Kirchhoff migration of reflection seismic data (Geoltrain and Brac, 1993). A good reflection image for complex media is only obtained, if first and later arrivals or most energetic arrivals are considered. In this case the resulting image displays the horizons with stronger amplitudes than an image generated with first arrivals.

For the high frequency data the traveltimes determined with the Eikonal solver match the most energetic events for most offsets (see Fig. 5). We can expect that a stack would provide the maximum amplitude at the correct position for these data since the moveout of the first arrival matches fairly well the moveout of the most energetic events in the seismograms. This is, however, not the case for the low frequency signal of Fig. 6. Obviously, several events are interfering in this case. The moveout of the computed first arrival traveltime does not correspond to the moveout of the interfering most energetic event in the seismogram. Since the moveout in the data is considerably larger this will lead to a maximum in the imagefunction for a source location at a smaller depth where the HF traveltime has a moveout similar to the event in the seismograms.

This assumption is now checked by the application of the diffraction stacking localization procedure to the synthetic data. For 60 Hz cut off frequency shown in Fig. 7 we see a distinct and unique maximum of the image function at the correct source location which is indicated by black lines in this and all following

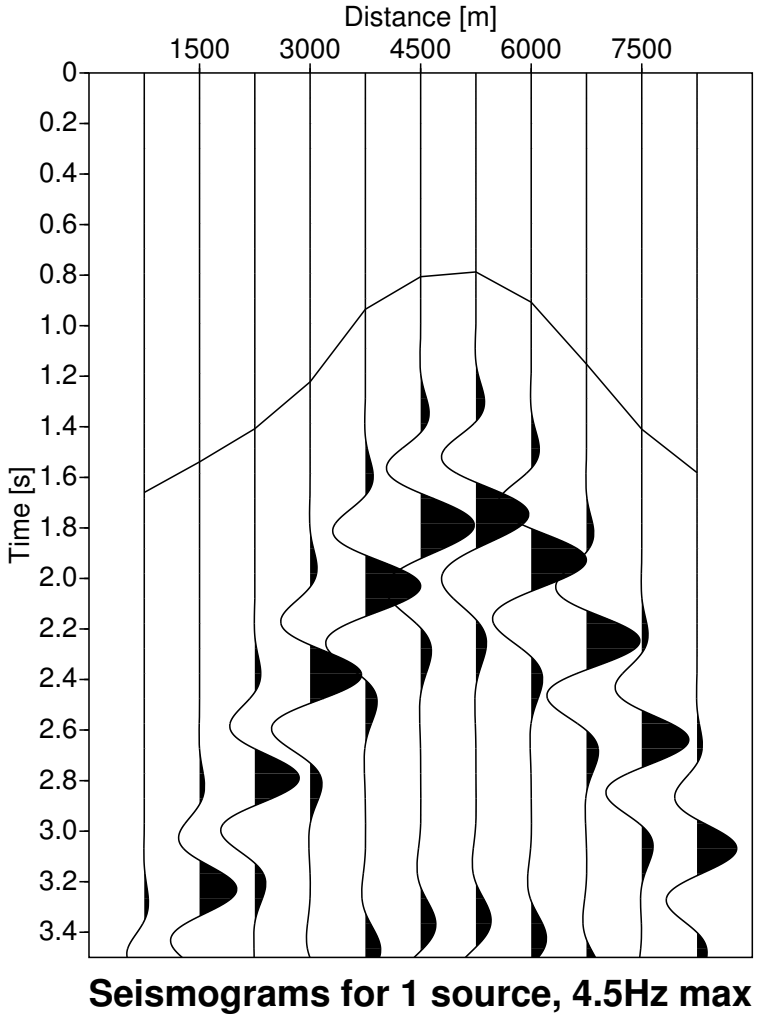

Figure 6: Seismograms for a point source in the acoustic heterogeneous medium (see Fig. 1). A Ricker signal is used as source time function with 4.5 Hz cut off frequency. First arrival traveltime curves for the correct source position and source time are also shown.

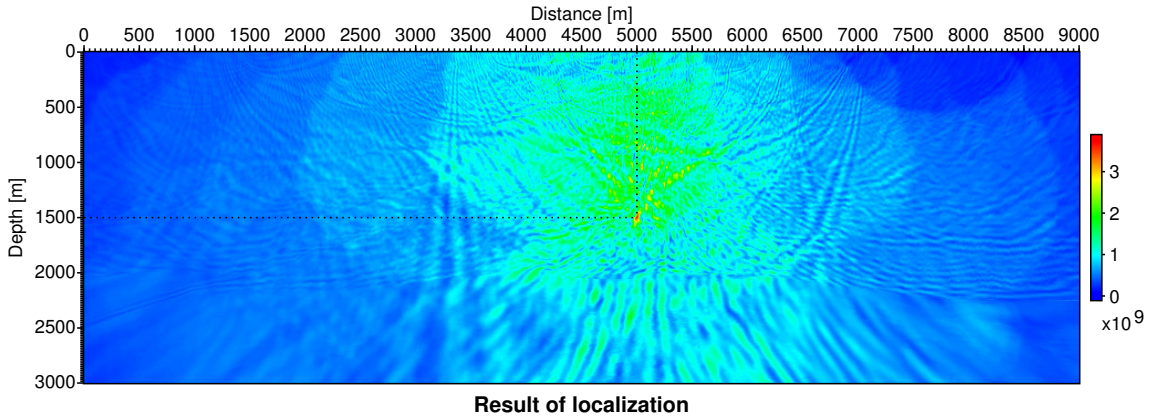

Figure 7: Localization of an explosive source (Ricker wavelet, 60 Hz cutoff frequency) in a heterogeneous acoustic medium. Colour legend on the right shows amplitude of the image function. The exact source location is indicated by dotted black lines.

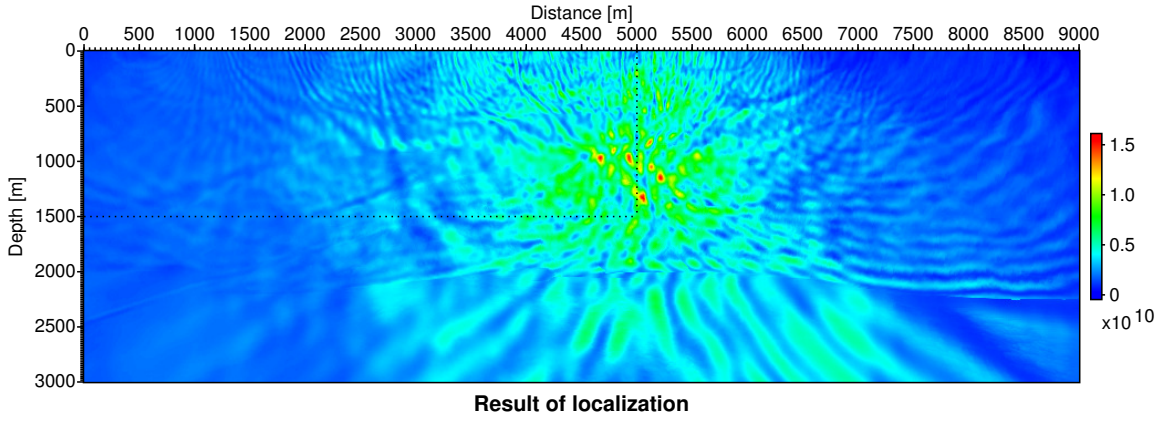

Figure 8: Localization of an explosive source (Ricker wavelet, 30 Hz cutoff frequency) in a heterogeneous acoustic medium. Colour legend on the right shows amplitude of the image function. The exact source location is indicated by dotted black lines.

figures of the image function. There is a large greenish area of higher amplitudes around the maximum which is caused by the sparse system of receivers in this example (just 11 receivers). An increase in the number of receivers would decrease the noise in the image function and enhance the amplitudes of the maximum of the image. For the data with 30 Hz cut off frequency shown in Fig. 8 the situation is different. Several spots with high amplitudes are present with the largest amplitude of the image function close to the exact source location. The maximum is located about 200 m upwards and about 100 m to the right of the exact location. For this example it would be difficult to decide which maximum really corresponds to the source location although the highest amplitudes are observed closest to the source. The spatial extent of this maximum is about twice the extent for the 60 Hz example.

For the signal with 4.5 Hz cut off frequency (Fig. 9) we again observe a distinct maximum with a spatial extent of about 1000 m (red area in Fig. 9) which corresponds approximately to the prevailing wavelength of this signal. The center of the maximum deviates by about 750 m from the exact source location. Since the HF first arrivals do not match the moveout of the data (Fig. 6) the maximum appears at a too small

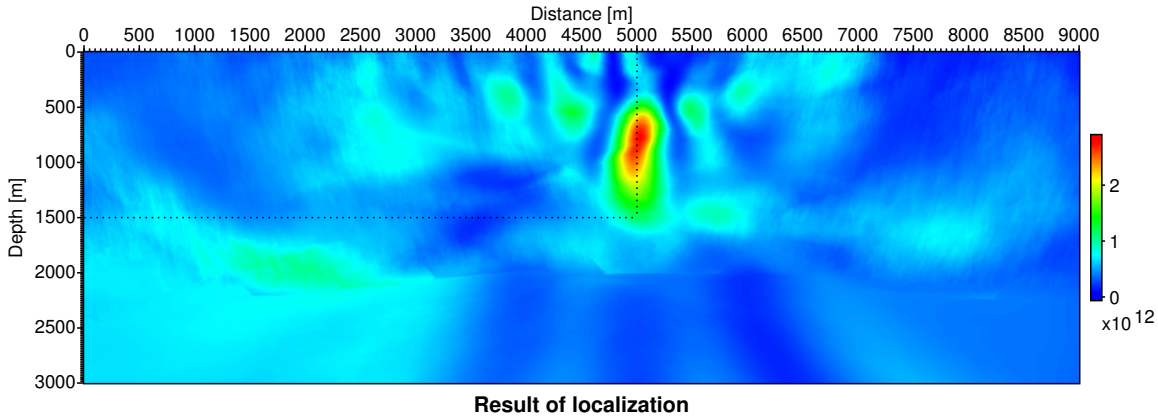

Figure 9: Localization of an explosive source (Ricker wavelet, 4.5 Hz cutoff frequency) in a heterogeneous acoustic medium. Colour legend on the right shows amplitude of the image function. The exact source location is indicated by dotted black lines.

depth. The moveout of the event is considerably larger than the moveout of the first arrival. For this example we obviously can not use HF first arrival traveltimes for localizing the event. In the next section we consider the same model but for the elastic case where an explosive point source is used. In this case we still have P-waves only but our wavefield is not a scalar one anymore but comprises the horizontal and vertical components of the displacement vector.

Elastic study

The elastic model corresponds to the model shown in Fig. 1 where the S-velocities are obtained from the P-wave velocities using a constant scaling factor of $1/\sqrt{2}$. The elastic forward modelling with the pseudo-spectral method generates seismograms for the horizontal and vertical component of the particle velocity. The type of the source used in this study corresponds to an explosive source. Therefore, only P-waves are generated. A Ricker signal with 4.5 Hz cutoff frequency is considered since the low frequency events are most relevant to simulate microtremor data. Seismograms and first arrival HF traveltimes for the exact source location and exact zero time for both components are shown in Fig. 10. Also for the elastic case we observe the difference in arrival times of the first arrival HF traveltimes and the arrival of maximum energy in the data. The explanation is as above: a combined effect of effective anisotropy and interfering later arrivals with the major impact by the latter.

The localization of the event using the stacking approach for the elastic data is shown in Figs. 11 and 12. The localization was applied to both components separately. The image functions for both localizations are scaled by the same factor and can be directly compared. The image function of the horizontal component has considerably smaller amplitudes than the vertical component which displays a distinc maximum with an extension of about 300m (red area). The center of the maximum is shifted upwards with respect to the exact source location. If we stack both image functions we obtain the result shown in Fig. 13 which does not differ very much from the result for the vertical component since its amplitudes are dominating. Compared to the acoustic data we obtain a more focused image function if elastic data are used.

From the numerical studies of this section we can conclude that the stacking approach to localize seismic events works for high frequency acoustic emission even in complex media and for a low number of receivers. More receivers would improve the amplitude of the image function and reduce the noise in the section. For low frequency events where the prevailing wavelength is smaller than the spatial extent of the complexities in the model localization errors are observed. The interference of events due to triplications change the moveout of the maximum energy arrival compared to the first arrival. Since the stacking trajectories are computed by an FD eikonal solver only high frequency first arrivals are modeled and a wrong

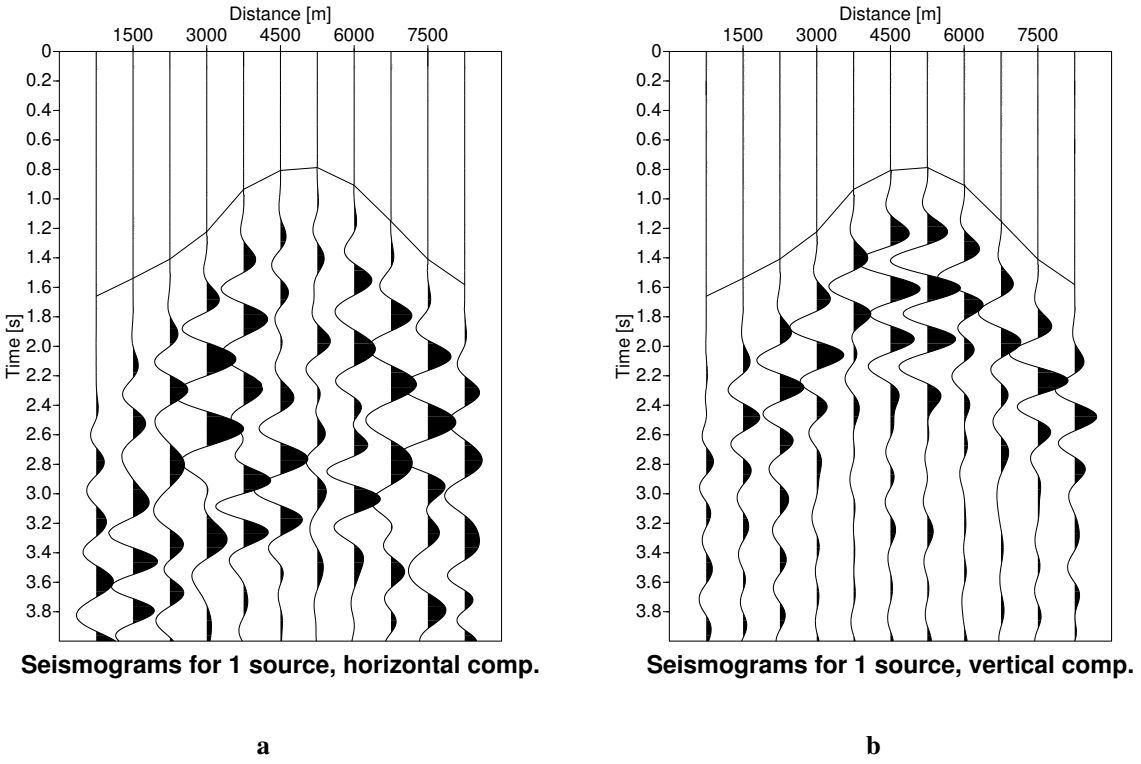

Figure 10: Seismograms for an explosive source in an elastic complex heterogeneous medium for horizontal (**a**) and vertical (**b**) component of particle velocity. A Ricker signal for 4.5 Hz cutoff frequency is used as a source signal. First arrival HF traveltime curves for the exact source position and source time are also shown.

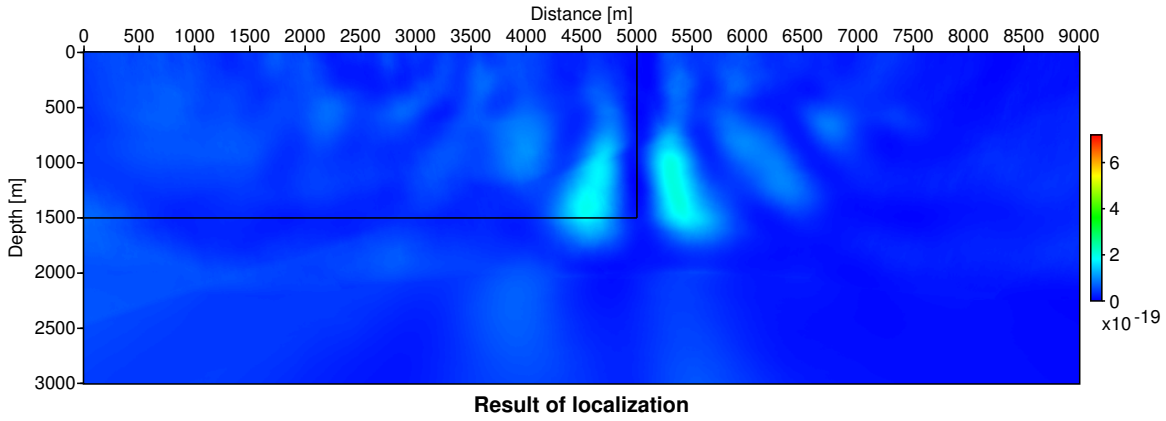

Figure 11: Localization of an explosive point source (horizontal component, 4.5 Hz cut off frequency Ricker wavelet) for a complex elastic medium. The color legend on the right shows the amplitude of the image function.

depth in the localization is obtained. For the localization of microtremor data this observation is significant since these events represent low frequency data. In the next section we apply the stacking approach for event localization to the synthetic microtremor data of Steiner et al. (2008b).

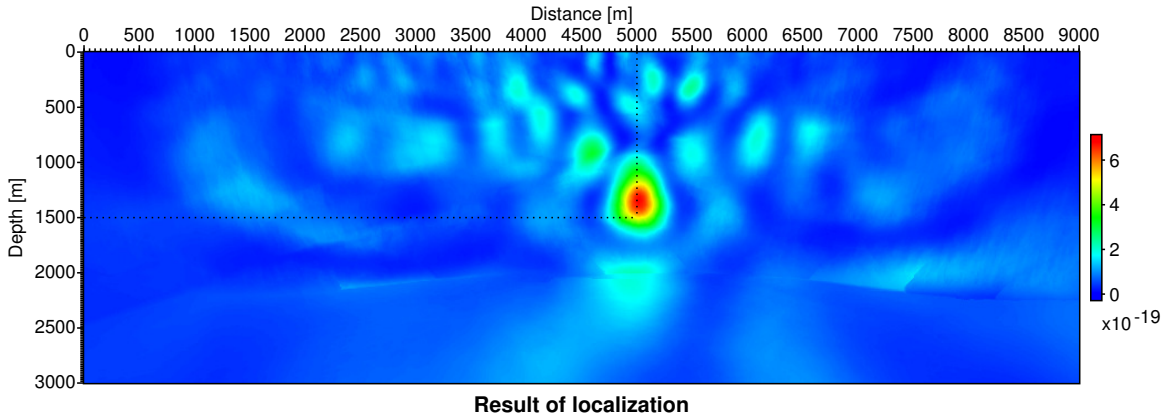

Figure 12: Localization of an explosive point source (vertical component, 4.5 Hz cut off frequency Ricker wavelet) for a complex elastic medium. The color legend on the right shows the amplitude of the image function.

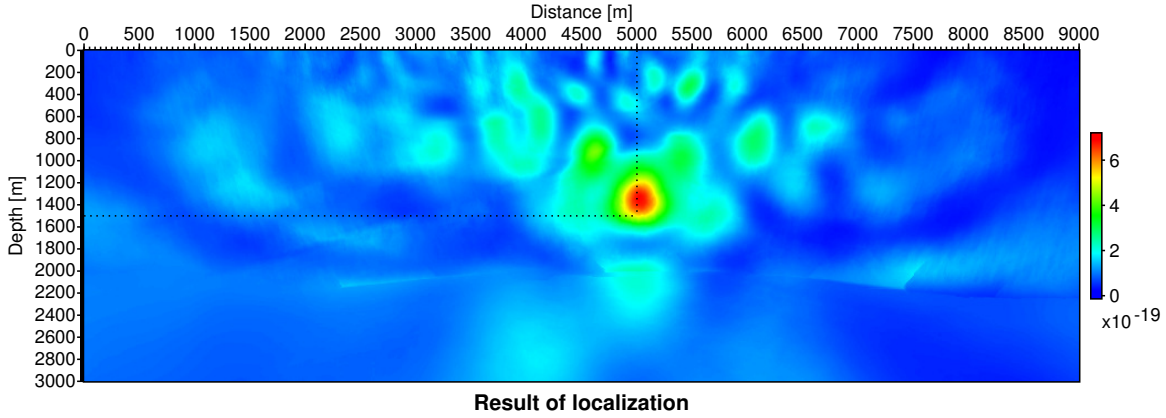

Figure 13: Localization of an explosive point source (stack of vertical and horizontal component, 4.5 Hz cut off frequency Ricker wavelet) for a complex elastic medium. The color legend on the right shows the amplitude of the image function.

NUMERICAL STUDY: MICROTREMORS

Microtremor data are different from impulsive seismic events like acoustic emissions (stationary signals). There is no first arrival for such kind of data. Microtremors produces continuous low-frequency "noise" signals (non-stationary signals). The diffraction stacking method should be applicable to microtremor data too since it considers all coherent energy at each time step. Thus, coherent energy should be imaged at the location it originated from. The synthetic microtremor dataset used here is the same as in the in work of Steiner et al. (2008b). A special forward modelling generates continuous microtremor signals similar to natural ones. Continuous microtremors are generated by applying 574 individual, short-time low-frequency sources with prevailing frequencies ranging between 1.5 Hz and 4.5 Hz (Ricker wavelet). These sources are randomly distributed within the reservoir zone (black lines in Fig. 1) and randomly distributed within the 108 seconds time window. The computations simulate the microtremor signal. The numerical time step is $2.9 \cdot 10^{-4}$ seconds. Horizontal and vertical particle velocities are computed throughout the time window for a recording network of 11 seismometers at the model surface. The acquisition is the same as for the

localization of the stationary signals as discussed in the previous section.

Steiner et al. (2008b) used two different types of sources in their simulations of microtremor signal. Synthetic microtremor data were generated using explosive point sources which generate only P-Waves. In another simulation Steiner et al. (2008b) used single force point sources to simulate the microtremor signal. In our study we consider only the first case, i.e., the microtremor signal is comprised of P-waves only. For this data no radiation correction need to be applied in the stack since an explosive point source has an isotropic radiation characteristic. Synthetic microtremor seismograms simulated from explosive point sources for the horizontal and vertical component of particle velocity are shown in Figs 14 a and b.

Localization by diffraction stacking was applied separately to the synthetic microtremor data for the horizontal and vertical components. As above, stacking trajectories are computed for the velocity model of Fig. 1 using an FD eikonal solver, i.e., the stack is performed for HF first arrival P-wave traveltimes. The resulting image functions are shown in Figs. 15, 16 respectively. As for the stationary data in the previous section, the amplitude of the image function for the horizontal component is considerably smaller than for the vertical component. A zone of high amplitudes is observed above the reservoir area where the lateral extent of this zone covers only the left part. The focal area of the image function represents the most likely distribution of microtremors and could be treated as the possible reservoir area. The center of the zone is about 300 m shallower than the reservoir zone. This coincides with the localization of low frequency stationary data where the location of the maximum of the image function was also shifted to shallower locations. The explanation here is the same as above. The model complexity combined with low frequency wave propagation leads to effective anisotropy and interfering high amplitude later arrivals with a different (i.e., larger) moveout than the moveout of the first arrival traveltimes. The stacking method for source localization thus obtains a maximum of the image function at a too shallow level.

In Fig. 17 we have stacked the image functions of the horizontal and vertical component. The resulting image, however, does not provide new insight into the localization. If we compare our results with the localization performed by Steiner et al. (2008b) using a reverse modeling approach for the localization we observe that the images obtained in our study show a much improved S/N ratio for shallow levels. This could be important for, e.g., shallow reservoirs. We can further conclude that the stacking approach for source localization is generally applicable to microtremor data. However, neither the depth nor the lateral extent are properly imaged by the current stacking approach. This may be improved by considering most energetic later arrival traveltime trajectories instead of first arrivals which is subject of an ongoing study.

CONCLUSIONS AND OUTLOOK

We have demonstrated in this study that the stacking approach for source localization is applicable to high frequency acoustic emissions even if the velocity model is complex and the observing receiver network is sparse. The stacking trajectories for these configurations are first arrival events which are easily generated by an FD eikonal solver. Limitations of the method are met when low frequency seismic events, or more precisely, events with a prevailing wavelength smaller than the spatial changes of the velocity model are considered. In this case the localization of sources is not correct even if the correct velocity is used to determine the first arrival stacking trajectories. For such data the most energetic events often originate by interference of several events due to triplications. These events display a different moveout than the first arrivals and are therefore stacked at a wrong depth.

In a later study we will compute HF later arrivals (i.e., most energetic arrivals) using ray tracing to test, whether we can better image the source position with these traveltime trajectories. It is known from Kirchhoff migration of reflection seismic data, that the inclusion of most energetic or later arrivals improve the image quality (Geoltrain and Brac, 1993, see, e.g.,). Here, however, the account of most energetic arrivals for the traveltime trajectories in the stack would not effect the stacking amplitude too much. The amplitudes are stacked by first arrivals too but for the wrong depth. Most energetic later arrivals display a different moveout and will stack the amplitudes for a different depth location. It is important to keep in mind, that the absolute traveltime in the stacking approach is not important for localization since we move the traveltime trajectory through the whole data window. As soon as coherent energy is present along the trajectory it contributes to the image function. The moveout of the stacking trajectory is the parameter which steers the localization and the moveout of later or most energetic arrivals is usually different from the moveout of first arrivals.

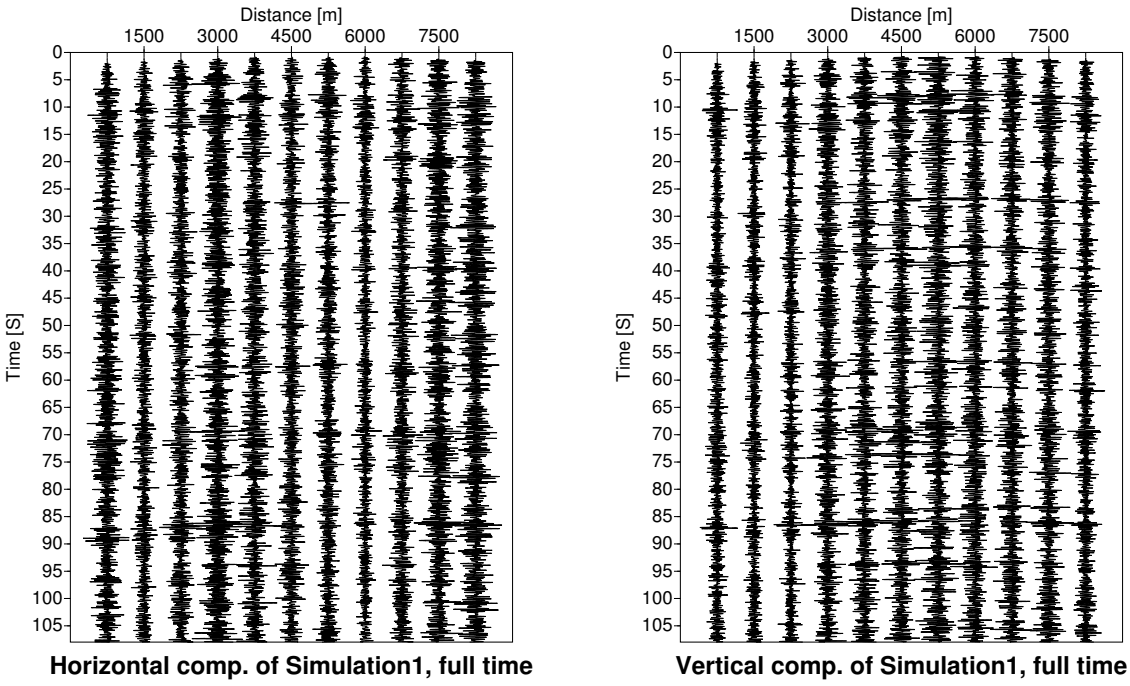

Figure 14: Synthetic seismograms simulating microtremor signals in a complex heterogeneous model (see Fig. 1). Horizontal component (a) and vertical component (b) of particle velocity are displayed.

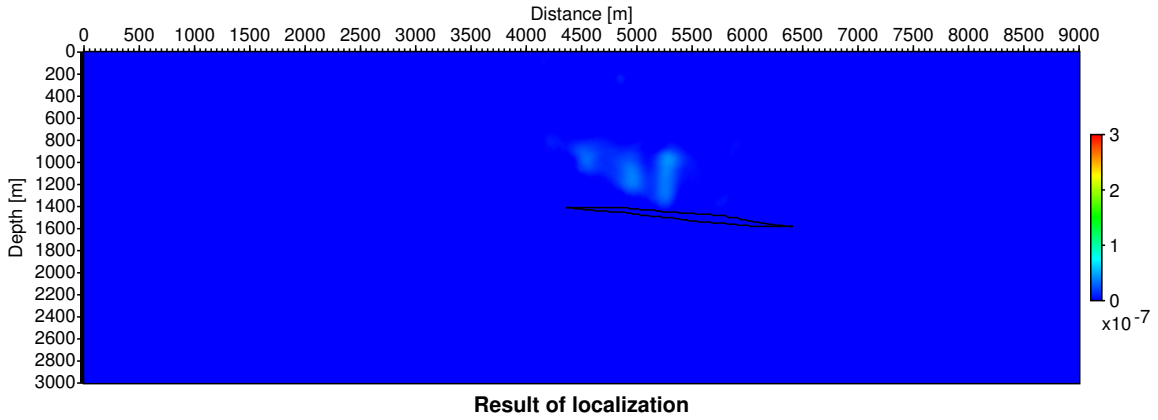

Figure 15: Image function of horizontal component for the localization of microtremors in a complex heterogeneous medium (see Fig. 1). The colour legend on the right shows amplitude of image function. The reservoir area is marked with black lines.

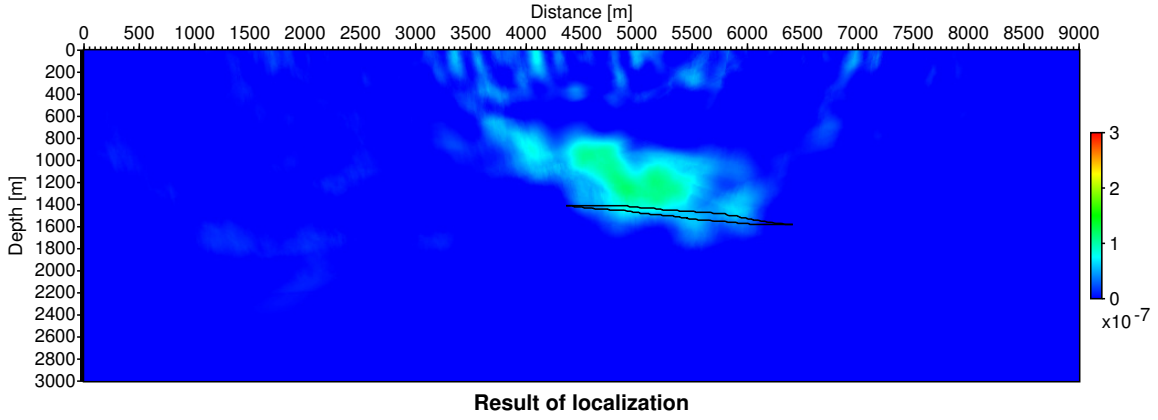

Figure 16: Image function of vertical component for the localization of microtremors in a complex heterogeneous medium (see Fig. 1). The colour legend on the right shows amplitude of image function. The reservoir area is marked with black lines.

Another factor contributing to changes in moveout is anisotropy which is controlled by, e.g., Thomsen's δ parameter. Even for this isotropic model effects of effective anisotropy may be present if the wavelength of the signal is considerably larger than the scale of heterogeneity in the model. This would, however, indicate that we are operating at the limit of the applicability of the ray method (Červený, 2001) for the complex isotropic model. This influence of effective anisotropy is very difficult to quantify since it depends on the model and the ray path. The δ parameter is usually not very large (about $0.1 - 0.2$) and thus influences the moveout not too much. Comparing the moveout of the first arrival traveltime in Fig. 6 with the actual moveout in the data it appears unlikely that effective anisotropy alone can account for this. It is most likely a combined effect of effective anisotropy and high energetic later arrivals with the stronger impact by the latter.

The localization of microtremor by the stacking approach appears principally possible. For complex models, however, the traveltime trajectories for the stack should comprise most energetic arrivals which display a different moveout than the first arrivals. The source images using the stacking approach have an improved S/N ratio for shallow levels when compared to other approaches for the localization of micro

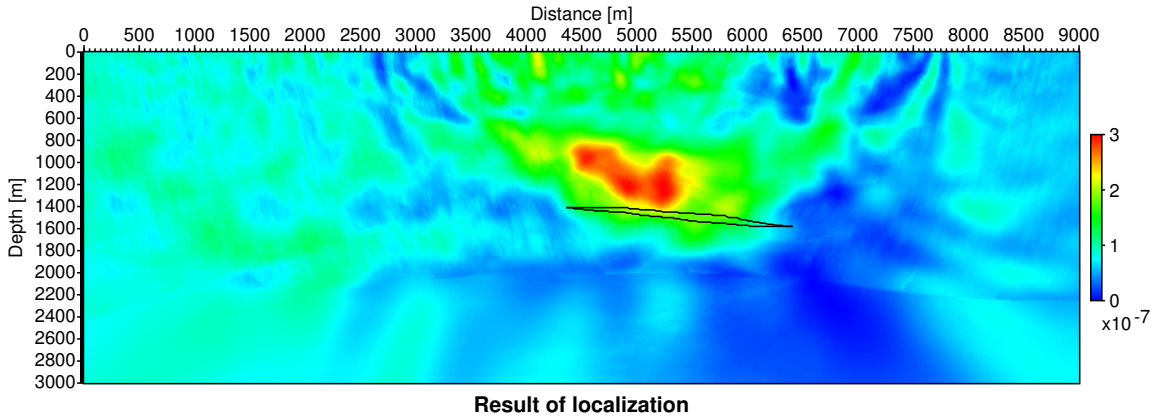

Figure 17: Stacked result of localizations for horizontal and vertical component of microtremors in a complex heterogeneous medium. The colour legend on the right shows the amplitude of the stacked image function. The reservoir area is marked with black lines.

tremors, like the reverse modeling approach. This can be of particular importance if shallow reservoirs are considered. Reverse modeling also requires a special imaging condition in order to map micro tremors which leads to some image processing Steiner et al. (2008a).

ACKNOWLEDGMENTS

We are grateful to Brian Steiner, ETH Zurich, Switzerland, who provided the model and the synthetic microtremor data. We also appreciate the valuable discussions with him on the localization of microtremors. We thank the Applied Geophysics Team in Hamburg, Germany and the Team of Elastic Media Dynamics Laboratory in St. Petersburg, Russia, for helpful discussions. This work was supported by the German Research Foundation (DFG, Ga350/14-1), the University of Hamburg, St. Petersburg State University, the DAAD (German Academic Exchange Service) and by the sponsors of the Wave Inversion Technology (WIT) Consortium.

REFERENCES

Anikiev, D., Gajewski, D., Kashtan, B., Tessmer, E., and Vanelle, C. (2006). Source localization by diffraction stacking. *10th Annual WIT report 2006*, pages 129–137.

Anikiev, D., Vanelle, C., Gajewski, D., Kashtan, B., and Tessmer, E. (2007). Localization of seismic events by a modified diffraction stack. *11th Annual WIT report 2007*, pages 13–25.

Červený, V. (2001). *Seismic Ray Theory*. Cambridge University Press.

Gajewski, D., Anikiev, D., Kashtan, B., Tessmer, E., and Vanelle, C. (2007). Localization of seismic events by diffraction stacking. In *Expanded Abstracts*, pages 1287–1291. Soc. Expl. Geophys.

Gajewski, D. and Tessmer, E. (2005). Reverse modelling for seismic event characterization. *Geophys. J. Int.*, 163:276–284.

Geoltrain, S. and Brac, J. (1993). Can we image complex structures with first arrival traveltime? *Geophysics*, 58:564–575.

Graf, R., Schmalholz, S. M., Podladchikov, Y., and Saenger, E. (2007). Passive low frequency analysis: Exploring a new field in geophysics. *World Oil*, 228:47–52.

Kosloff, D. and Baysal, E. (1982). Forward modeling by a fourier method. *Geophysics*, 47:1402–1412.

Leidenfrost, A., Ettrich, E., Gajewski, D., and Kosloff, D. (1999). Comparison of six different methods for calculating traveltimes. *Geophys. Prosp.*, 47:269–297.

Rentsch, S., Buske, S., Lüth, S., and Shapiro, S. (2007). Fast location of seismicity: A migration-type approach with application to hydraulic-fracturing data. *Geophysics*, 72(1):S33–S40.

Reshef, M., Kosloff, D., Edwards, M., and Hsiung, C. (1988). Three-dimensional acoustic modeling by the fourier method. *Geophysics*, 53:1175–1183.

Steiner, B., Saenger, E., and Schmalholz, S. (2008a). Case studies on time reverse modeling of low-frequency microtremors. In *EAGE Expanded Abstracts*.

Steiner, B., Saenger, E., and Schmalholz, S. (2008b). Time reverse modeling of low-frequency microtremors: Application to hydrocarbon reservoir localization. *Geophys. Res. Let.*, 35:L03307.

Vidale, J. (1988). Finite-difference travel time calculation. *Bull. Seism. Soc. Am.*, 78:2062–2076.